Polyelectrolyte Coupling to a Charged Lipid Monolayer

Kerstin de Meijere,* Gerald Brezesinski, and Helmuth Möhwald

Max-Planck-Institut für Kolloid- und Grenzflächenforschung, Rudower Chaussee 5, D-12489 Berlin, Germany

Received October 8, 1996; Revised Manuscript Received January 27, 1997[⊗]

ABSTRACT: The interaction of a positively charged polyelectrolyte with the negatively charged 1,2-dipalmitoylphosphatidic acid monolayer at the air/water interface is studied by film balance, fluorescence microscopy, and surface X-ray diffraction measurements. It is shown that polymer binding leads to a local lattice expansion without insertion into the film at high lateral pressure (>20 mN/m). The film exhibits a rectangular structure with uniform chain tilt. The tilt angle decreases slightly with increasing lateral pressure. This contrasts with the film in the absence of polymer where a structure sequence oblique → rectangular → hexagonal was found. At low lateral pressures, the polyelectrolyte/lipid film shows coexistence of ordered and disordered regions with inhomogeneities gradually removed on pressure increase. The uniformity of the lipid/polyelectrolyte interaction is manifested in distinct and narrow diffraction peaks.

Introduction

Langmuir monolayers of charged lipids coupled to oppositely charged polyelectrolytes are of great interest for a variety of reasons: They represent well-defined model systems to study the interface between an amphiphile and a polymer, because molecular density and charge density of both components and the ionic milieu can be manipulated to a large extent in a well-defined way. This interface is of high relevance for many biophysical membrane problems[1] as well as technical systems where mechanical strength of the polymer[2] and the selective barrier characteristics of a lipid double layer shall be coupled. From a basic physical point of view, the most interesting question concerns the interplay between lateral forces of the lipids and entropic forces of a flexible polymer. In the specific situation of the polyelectrolyte/lipid coupling, this involves the following question: Which influences dominate when a polyelectrolyte binds to a charged surface, the reduction of Coulomb repulsion of the ionic head groups causing an increase of the lateral lipid density or the entropic forces of the polymer causing reduced density and disorder? A very sensitive means of measuring this interplay is to study shifts of phase transitions and, more specifically, phase diagrams.

Looking at literature data of shifts of phase transitions from the liquid expanded (LE) to the liquid condensed (LC) phase of Langmuir monolayers or the gel to liquid-crystal transition of bilayers reveals that an answer to this question will depend on the system: Coupling of polyethyleneimine to fatty acid monolayers tends to stabilize the LE phase;[3] polypeptides and proteins electrostatically bound favor the gel phase of bilayers.[4] The polyelectrolyte poly(diallyldimethylammonium chloride) (PDADMAC) increases the melting temperature of dihexadecylphosphate bilayers.[5] In the case of special polymerizable lipids, the melting points of polymerized vesicles are shifted toward lower temperatures compared to the corresponding monomeric vesicles, which is explained by a disordering influence of the polymer chain on the head group packing.[6] These results indicate that we are far from a quantitative understanding, and more systematic studies are needed.

Serious problems with these experiments concern equilibrium and nonequilibrium features, hysteresis, and inhomogeneities. These require studies of different time and length scales. As a start, in this work we investigate monolayers at long times (hours) and short length scales by X-ray diffraction. The lipid chosen is a phospholipid (DPPA) that also forms a stable monolayer after polymer coupling. The polyelectrolyte is PDADMAC, exhibiting a well-known charge density along its flexible linear chain. We show that stable and homogeneous films can be formed with entropic forces strongly influencing the phase diagram.

Experimental Section

1. Materials. The L-1,2-dipalmitoylphosphatidic acid (purity 98 %) was purchased from Sigma (Taufkirchen, Germany) and spread from a 10^{-3} M solution in chloroform (Merck, Germany, p.a. grade) onto an ultrapure water subphase. Purification of the water in a Millipore desktop filtering system leads to a specific resistance of 18.2 MΩ cm.

PDADMAC was kindly synthesized by Antje Wenzel (MPI f. Kolloid und Grenzflächenforschung, Teltow, Germany)[6] using a synthesis that gives an un-cross-linked, linear polymer material in which the repeat unit mainly consists of a five-membered-ring species. The batch used in the experiments had a molecular weight of $M_n = 76{,}000$. It was added to the water subphase in a concentration of 10^{-3} M (referring to the molecular weight of one monomer unit) before spreading the monolayer solution. After spreading the lipid monolayer, the polymer was given ∼30 min to adsorp. Longer adsorption times up to 8 h did not change the isotherm. The chemical structures of the two substances are shown in Figure 1.

2. Methods. The pressure/area isotherms were measured on a thermostated film balance (R&K, Germany) equipped with a Wilhelmy system to continuously record the surface pressure during the compression of the monolayer.

Fluorescence microscopic images were obtained with a Zeiss Axiotron microscope using a long-distance objective ($d = 8$ mm). The fluorescence dye L-α-phosphatidylcholine-β-[*N*-(7-nitrobenz-2-oxa-1,3-diazol-4-yl)aminohexanoyl]-γ-palmitoyl (1 mol %) (Sigma) was added to the spreading solution. Its emission is excited by a 50-W Hg high-pressure lamp via a dichroic mirror and detected by means of a SIT camera (Hamamatsu C2400). Images were recorded by a video recorder and then digitized and analyzed with NIH Image 1.60.[7]

The Synchrotron X-ray experiments at grazing incidence (GID) were carried out on the liquid surface diffractometer at the undulator beam line BW1 at HASYLAB, DESY (Hamburg,

[⊗] Abstract published in *Advance ACS Abstracts,* March 15, 1997.

S0024-9297(96)01490-8 CCC: $14.00

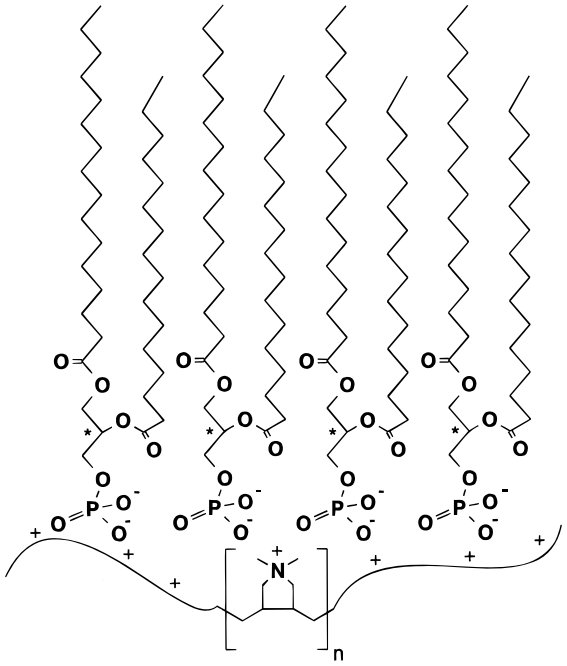

Figure 1. Chemical structures of the lipid L-1,2-dipalmitoylphosphatidic acid and the polyelectrolyte poly(diallyldimethylammonium chloride). The asterisk marks the asymmetric carbon atom (chiral center).

Germany).[8] The Synchrotron beam was made monochromatic by Bragg reflection by a beryllium (002) crystal and was adjusted to strike the monolayer on the water surface at an angle of incidence $\alpha_i = 0.85\alpha_c$, where α_c is the critical angle of total external reflection. The intensity of the diffracted radiation is detected by a position-sensitive detector (PSD) (OED-100-M, Braun, Garching, Germany). The resolution of the horizontal scattering angle $2\theta_{hor}$ is given by a Soller collimator located in front of the PSD. The scattering vector **Q** has an in-plane component $Q_{xy} = (4\pi/\lambda)\sin(2\Theta_{hor}/2)$ and an out-of-plane component $Q_z = (2\pi/\lambda)\sin\alpha_f$, where λ is the X-ray wave length and α_f the vertical scattering angle. The accumulated position-resolved scans were corrected for polarization, footprint area, and powder avaraging (Lorentz factor). The intensities of the diffraction peaks were least-squares fitted to model peaks as products of a Lorentzian parallel and a Gaussian normal to the water surface.[9−12]

The lattice spacings are obtained from the in-plane diffraction as

$$d_{hk} = 2\pi/Q_{xy}^{hk} \tag{1}$$

The lattice parameters a and b can be calculated from the lattice spacings, and the unit cell area A_{xy} is calculated from the lattice parameters.

If two diffraction maxima occur, the monolayer forms a centered rectangular lattice where the tilt azimuth can be in one of the two symmetry directions, toward the nearest neighbor (NN) or toward the next nearest neighbor (NNN). In the case of a NN tilt direction, the maximum of the 2-fold degenerate peak Q_{xy}^d occurs at $Q_z^d > 0$ Å^{-1} and that of the nondegenerate peak at $Q_z^n = 0$ Å^{-1}. The tilt angle is then given by

$$t = \arctan \frac{Q_z^d}{\sqrt{(Q_{xy}^d)^2 - (Q_{xy}^n/2)^2}} \tag{2}$$

Three nondegenerate diffraction maxima at $Q_z > 0$ Å^{-1} are measured if the unit cell has an oblique symmetry with three different lattice spacings.

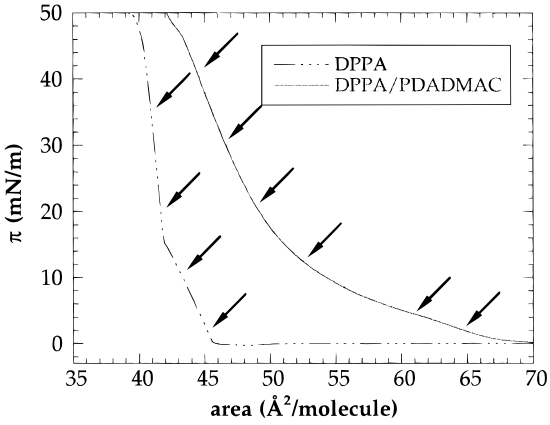

Figure 2. Surface pressure π as a function of molecular area for a monolayer of DPPA and DPPA on PDADMAC at 20 °C. The arrows indicate the surface pressures at which diffraction data have been taken.

Once the tilt angles are determined, the cross-sectional area of the chains is given by

$$A_0 = A_{xy}\cos(t) \tag{3}$$

Assuming an exponential decay of positional correlations with increasing separation within the layer, the full width at half-maximum $\Delta_{int}(Q_{xy})$ corrected for resolution effects of the detector can be taken to determine the positional correlation length ξ:

$$\xi = \frac{2}{\Delta_{int}(Q_{xy})}$$

3. Results and Interpretation

Figure 2 compares pressure/area isotherms of DPPA with those of DPPA coupled to the polyelectrolyte. The presence of the polyelectrolyte at the interface was additionally verified by ellipsometry and X-ray reflectivity, which will be published separately. The DPPA isotherm is typical for many lipids and fatty acids with sufficiently strong van der Waals attraction to prevent a liquid expanded phase. In this case, the onset of the lateral pressure π upon compression, occurring at ∼46 Å^2/molecule, corresponds to the formation of an ordered phase with uniform chain tilt.[13] With increasing π, the tilt angle is reduced and the break in the slope near 15 mN/m indicates the formation of a phase where the tilt angle is independent of pressure. The isotherm with PDADMAC bound to DPPA is more expanded and exhibits less pronounced features. There is a slight but reproducible change in the slope near 5 mN/m which will be discussed later.

The X-ray diffraction data given in Figure 3 as contour plots (intensity as a function of in-plane and out-of-plane scattering vector components) for DPPA monolayers at different lateral pressures enable more quantitative and refined conclusions than given above from the isotherms. At the lowest pressure, one observes three distinct diffraction maxima for 1.43 Å$^{-1} \leq Q_{xy} \leq$ 1.49 Å^{-1}, indicative of an oblique chain lattice. The existence of maxima with $Q_z > 0$ Å^{-1} proves a uniform aliphatic chain tilt. The same interpretation holds also for the measurement at 10 mN/m, although there the three maxima strongly overlap and can be deduced only by deconvolution. The fact that there are indeed three maxima is derived from the finding that it is impossible to simulate the contour with only two

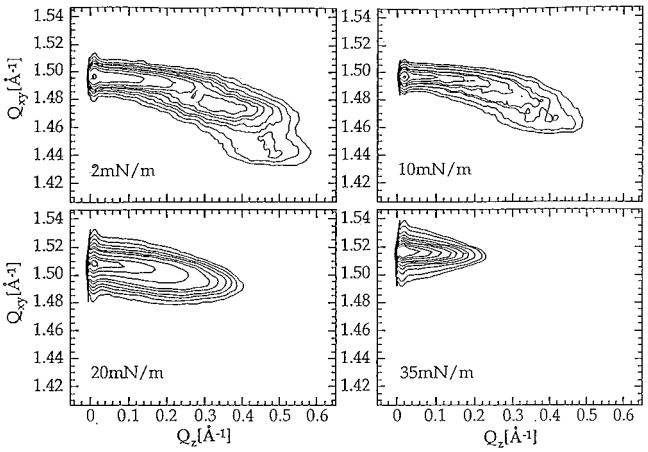

Figure 3. Contour plots of the corrected X-ray intensities as a function of the in-plane component Q_{xy} and the out-of-plane component Q_z of the scattering vector **Q** of DPPA monolayers at different lateral pressures.

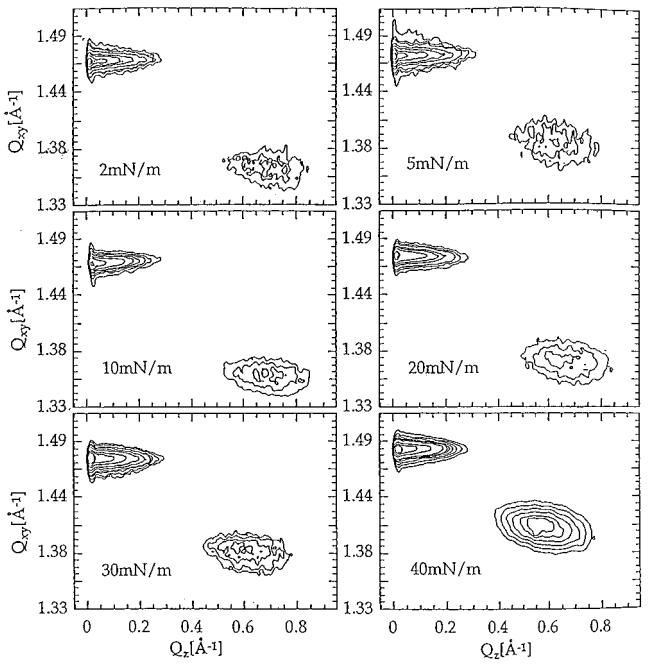

Figure 4. Contour plots of the corrected X-ray intensities as a function of the in-plane component Q_{xy} and the out-of-plane component Q_z of the scattering vector **Q** of DPPA monolayers on a PDADMAC subphase at different surface pressures.

peaks of reasonable shape in Q_{xy} and Q_z. The latter, however, is possible for the measurement at 20 mN/m where again the large width in Q_z proofs that there are two maxima, one with $Q_z = 0$ Å^{-1} and one with $Q_z \approx 0.17$ Å^{-1}. This signifies a rectangular lattice with nearest-neighbor tilt.[10,11] Hence, between 10 and 20 mN/m there is a phase transition from an oblique to a rectangular lattice and very probably this is related to the slope change in the isotherm near 15 mN/m. Not detectable in the isotherms is another transition into a hexagonal phase, the existence of which is indicated by the measurement of only one diffraction peak at 35 mN/m. The fact that the maximum occurs at $Q_z = 0$ Å^{-1} reveals that the aliphatic tails are not tilted.

DPPA on a polyelectrolytic subphase gives qualitatively different X-ray data (Figure 4). At all pressures there is one peak with $Q_z = 0$ Å^{-1} and one with $Q_z > 0$ Å^{-1}, indicative of a rectangular lattice with nearest-neighbor tilt. The latter peak, as expected, shifts toward higher Q_{xy} and lower Q_z with increasing pressure, but this shift is less pronounced than in the absence of polyelectrolyte.

The fluorescence microscopy observations at low and at medium pressures (Figure 5) reveal that the monolayer is heterogeneous with disordered regions containing the fluorescence probe and ordered regions excluding it. On increasing the pressure, the area fraction of ordered regions increases, however with large local variations probably caused by pressure heterogeneities. By increasing the pressure above 20 mN/m, the contrast disappears and the surface is almost exclusively coated by dark (ordered) areas.

Analysis, Discussion, and Conclusions

Table 1 gives data derived from analysis of the diffraction measurements. In order to compare parameters for the three different lattices, we used indexing for the lattice of lowest symmetry, the oblique one. Common to all measurements is the cross section per chain of (20.0 ± 0.3) Å^2; i.e., in all ordered structures the lipids are in the "free rotator" phase. This is to be distinguished from the crystalline phases of fatty acids with cross sections below 19 Å^2,[14] and indeed, the measured line widths are broader than resolution limited.

The measurements on DPPA monolayers in the absence of polyelectrolyte were intended only as a reference. In connection with data on other phospholipids, however, they also yield new information on lipid arrangement. An oblique lattice was previously found for monolayers of enantiomers with the phosphatidylethanolamine head group[15] or with the phosphatidylcholine head[12] and ascribed to hydrogen bonding and to packing problems within the phosphatidylcholine moiety, respectively. Here we have an oblique lattice for the smallest possible phospholipid head with no hydrogen bonding. Hence, we must invoke a local interaction of the chiral glycerophosphate leading to a chiral (oblique) structure. This requires orientational order of the heads and packing constraints by head group interactions. The latter are obviously removed upon compression such that the density is determined by chain packing.

We note that the projected molecular areas A_{xy} are similar to those given by the isotherms. This indicates a negligible fraction of less dense (not diffracting) monolayer regions between domains of ordered structure. We also note that, in contrast to findings with fatty acids,[13] the isotherm slope change at 15 mN/m does not correspond to a transition into an untilted phase. In addition, the two tilted phases involved in the transition do not seem to be distinguished by a lateral compressibility[16] of more than a factor of 2. The factor is derived from X-ray data as well as from pressure/area isotherms. This indicates that the compressibility is due to a change in local interactions of the ordered phase not due to a change in the area fraction of the still existing disordered regions. Most probably there is a change in the arrangement of the hydrophilic head groups involved.

The data with PDADMAC bound to DPPA enable many important conclusions:

(I) The diffraction pattern gives no indication of contributions from patches of monolayer not bound to polymer. Since their peaks would be distinct, they would be detected if their area fraction was above 10%. Hence, there is virtually no polymer free film.

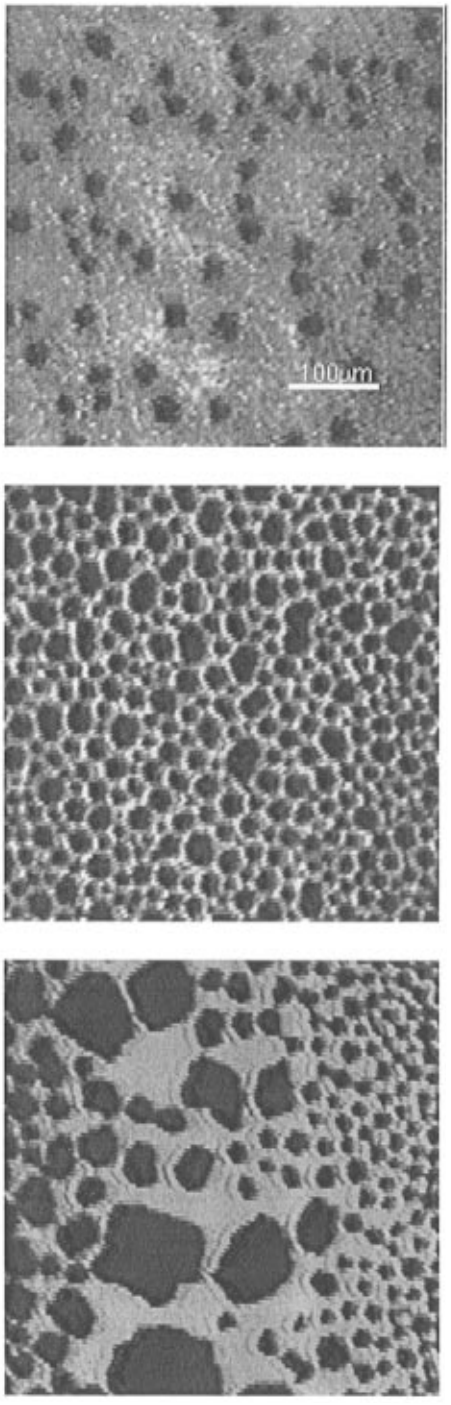

Figure 5. Fluorescence micrographs of a DPPA monolayer, containing 1 mol % of a fluorescence dye, on PDADMAC at different lateral pressures.

(II) Inspecting the positional correlation lengths ξ_i, we note that they are much shorter into the direction of the tilt azimuth than perpendicular to it. This is a general phenomenon with Langmuir monolayers and has been ascribed to a one-dimensional crystallization[17] and to a weaker interaction along the tilt direction. Now comparing the correlation lengths in the absence or presence of polyelectrolyte for the tilted rectangular phase (at the same lateral pressure but at different tilt angles), it is interesting to note that the presence of the polymer enlarges them perpendicular to the tilt direction but makes them smaller into the tilt direction. The ratio between the correlation lengths into these two direction increases from 2:1 in the absence of polymer to 6:1 in the presence of polymer. This demonstrates that the polymer improves the one-dimensional crystallization perpendicular to the tilt direction and creates distortions into the tilt direction. The uniformity of the system on these length scales requires that the interactions between the condensed monolayer and the polyelectrolyte, averaged over ~200 Å are identical across the measured area of 50 mm^2 and also that no polyelectrolyte is inserted into the condensed monolayer. The latter would lead to strong line broadening in contrast to the observations.

Table 1. Unit Cell Parameters *a*, *b*, and γ and Projected Area per Chain A_{xy}, As Derived from In-Plane Diffraction Data, Cross-Sectional Area A_o, Tilt Angle *t*, and Positional Correlation Lengths ξ_i, As Derived from the Full Width at Half-Maximum of the In-Plane Diffraction Peaks, at Different Surface Pressures[a]

(a) DPPA

π (mN/m)	*a* (Å)	*b* (Å)	γ (deg)	*t* (deg)	A_{xy} (Å^2)	A_o (Å^2)	ξ_1 (Å)	ξ_2 (Å)	ξ_3 (Å)
2	4.87	4.98	118.4	19	21.4	20.2	99	67	54
10	4.86	4.90	118.8	14	20.9	20.3	127	68	68
20	4.87	4.82	120.2	8	20.3	20.2	143	87	
35	4.79	4.79	120	0	19.8	19.8	280		

(b) DPPA on PDADMAC

π (mN/m)	*a* (Å)	*b* (Å)	γ (deg)	*t* (deg)	A_{xy} (Å^2)	A_o (Å^2)	ξ_1 (Å)	ξ_2 (Å)	I_1 (au)
2	5.47	5.08	122.6	31	23.4	20.2	205	30	1410
5	5.35	5.04	122.1	28	22.8	20.2	205	35	1340
10	5.50	5.08	122.8	31	23.5	20.2	235	80	1840
20	5.40	5.05	122.3	29	23.1	20.2	180	30	2560
30	5.36	5.03	122.2	28	22.8	20.1	180	35	3480
40	5.21	4.98	121.5	25	22.1	20.0	180	40	3840

[a] I_1 represents the corrected scattering intensity of the nondegenerated diffraction peak.

(III) Protrusion of polyelectrolyte into the hydrophobic region at pressures of >20 mN/m can also be excluded from the near-identity of projected molecular areas and those derived from the isotherms; e.g., at 20 mN/m the area per molecule derived from X-ray studies, 2 × 23.1 Å^2 = 46.2 Å^2, is very close to the value according to the π/A isotherm. This conclusion does not necessarily hold at lower pressures where the molecular areas derived by X-ray studies are considerably smaller than those derived from the isotherms. This can be due to polyelectrolyte inserting into the monolayer but also due to the presence of lipid in a disordered phase (the molecular areas of double-chain phospholipids in the LE phase range from 60 to 100 Å^2).[18]

(IV) The comparison with LE phase monolayers, however, is very problematic because the films are highly viscous. This is probably why also at a pressure as low as 2 mN/m, i.e., below the slight slope change, a diffraction signal is observed. For a crude estimate of the lipid fraction in the ordered phase, we may use the measurements of the integrated intensities.

The latter are a factor of ~2 smaller at the lowest pressures compared to the highest ones. Neglecting changes in the Debeye−Waller factor, justified by the finding that other parameters like lattice parameters, line width, and tilt angles are not qualitatively different, we may deduce that half of the lipids are in the ordered phase. The area per lipid in the disordered regions A_d can then be deduced according to

$$A = \frac{1}{2}A_o + \frac{1}{2}A_d$$

with *A* the molecular area derived from the isotherm

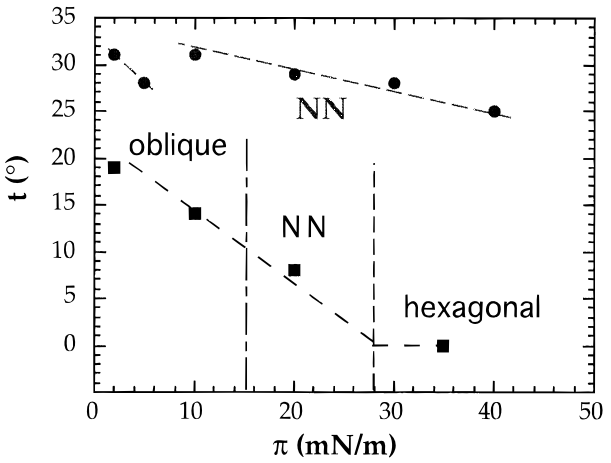

Figure 6. Tilt angle *t* as a function of pressure for DPPA (■) and DPPA on PDADMAC (●). The phase sequences are indicated.

and $A_o = 2A_{xy}$ the molecular area derived from X-ray diffraction. We obtain for the data at 2 mN/m

$$A_d = 2A - A_o = (126-47)\ \text{Å}^2 = 79\ \text{Å}^2$$

This value is still within expectations for a disordered lipid; thus, we can neither prove or disprove the insertion of polymer into the monolayer. In any case, the data show that the monolayer is heterogeneous for $\pi <$ 10 mN/m.

(V) Figure 6 compares the tilt angle *t* as a function of surface pressure in the absence and presence of polyelectrolyte. One clearly observes that polyelectrolyte binding leads to a decrease of lateral lipid density, and to optimize van der Waals interaction, the lipid responds by an increase of the tilt angle. This most important result will be discussed at length at the end. For the polyelectrolyte-coupled monolayer, one realizes that the two measurements at 2 and at 5 mN/m do not follow the expected monotonic behavior. This is probably due to a heterogeneous lateral pressure distribution that is removed at sufficiently large lateral pressure. Very probably the latter pressure corresponds to the isotherm slope change near 5 mN/m. Since this heterogeneity is related to the polymer coupling, one can suggest, but not prove, that polymer inserted into the film causes the heterogeneity and it is removed by a pressure increase. It is also remarkable that the integrated intensity increases most drastically above a pressure of 5mN/m, presumably due to an increase of the ordered lipid fraction.

An alternative explanation for the slope change could be a glass transition of the disordered lipid regions coupled to the polymer, as has been observed for monolayers of amphiphilic polymers.[19] This may be related to a polyelectrolyte rearrangement effectively changing its extension into the water and thus contributing to the lateral compressibility.

(VI) The experiments have shown that polyelectrolyte coupling leads to monolayer expansion at the molecular level without polyelectrolyte insertion into the monolayer. We therefore conclude that entropic repulsion exceeds the screening of Coulomb forces on binding. This conclusion also holds for fatty acid monolayers coupled to polyelectrolytes, because previous isotherm and fluorescence microscopic studies[3] and also our similar X-ray analysis (to be published) support it. Both systems, however, are unsuited for a quantitative determination of forces, because they exhibit no LE/LC transition in the absence of polyelectrolyte. More experiments dedicated to a quantitative understanding, also varying the ionic milieu, are underway.

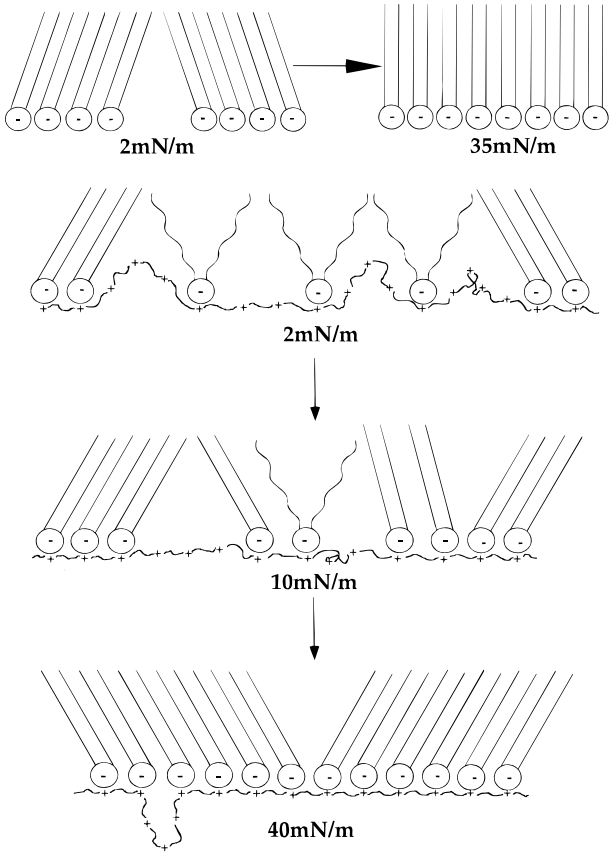

Figure 7. Schematic representation of the molecular arrangement in a DPPA monolayer (first row) and in a DPPA monolayer on the polyelectrolyte PDADMAC at different lateral pressures.

(VII) We also note that polymer coupling not only leads to expansion but to a removal of the oblique as well as the hexagonal lattice. This is probably due to a decoupling of the head groups and destruction of head group lattice that was assumed to be responsible for a chiral structure. The hexagonal lattice on the other hand requires a denser chain packing than is possible in this situation.

(VIII) We should also make some remarks about scanning force microscopy (SFM) data of subdomains of 0.1 μm size within the micrometer-sized domains observed by fluorescence microscopy.[20] We have shown here that the structure of the lipid layer with coupled polyelectrolyte changes with surface pressure, and changes would also be observed upon transfer on a solid support after the loss of water. This would yield a lateral shrinking, but due to the polymer coupling, the transport would be inhibited. This should yield small ordered phase domains separated by clefts, as observed by SFM, but by no means will represent the monolayer at the air/water interface.

Altogether, the picture of the pressure-dependent structure can be visualized as depicted in Figure 7. In the absence of polyelectrolyte, the monolayer exhibits an ordered structure with uniform tilt and some monolayer free areas between ordered phase domains. The tilt angle decreases with increasing pressure, and the lattice changes from oblique via rectangular to hexagonal. The polyelectrolyte coupling causes a lattice ex-

pansion, a rectangular lattice, and a tilt at all pressures. At low pressure there is coexistence between an ordered and a disordered state and the polyelectrolyte protrudes possibly into the disordered, not into the ordered state. Near 5 mN/m lateral inhomogeneities are progressively removed, and near 20 mN/m the monolayer is in a homogeneous phase. It is not clear at this point whether the whole polymer chain is stretched underneath the monolayer or whether it also forms loops at high lateral pressure. The tilt angle cannot be lowered toward zero, and even at 40 mN/m it is larger than in the absence of polymer near 2 mN/m. In addition, the coupling favors the existence of a rectangular phase. The well-defined structure of the polyelectrolyte-coupled monolayer is probably also related to the 1:1 stoichiometry of the lipid/polymer coupling.[21]

Acknowledgment. We thank HASYLAB at DESY, Hamburg, Germany, for beam time and providing excellent facilities and support. The inspiring collaboration with K. Kjaer, especially his help with setting up the X-ray experiment, is gratefully acknowledged.

References and Notes

(1) McLaughlin, S. A. *Curr. Top. Membr. Transp.* **1977**, *9*, 71.
(2) Shimomura, M.; Kunitake, T. *Polym. J.* **1984**, *16*, 187.
(3) Chi, L. F.; Johnston, R. R.; Ringsdorf, H. *Makromol. Chem., Makromol. Symp.* **1991**, *46*, 409.
(4) Maksymiw, R.; Sen-fang, S.; Gaub, H.; Sackmann, E. *Biochem.* **1987**, *26*, 1017.
(5) Antonietti, M.; Kaul, A.; Thünemann, A. *Langmuir* **1995**, *11*, 2633.
(6) Bader, H.; Dorn, K.; Hupfer, B.; Ringsdorf, H. *Adv. Polym. Sci.* **1985**, *64*, 1.
(7) Thoma, M.; Möhwald, H. *J. Colloid Interface Sci.* **1994**, *162*, 340.
(8) Kjaer, K.; Majewski, J.; Schulte-Schrepping, H.; Weigelt, J. *HASYLAB Annu. Rep.* **1994**, 589.
(9) Als-Nielsen, J.; Möhwald, H. In *Handbook on Synchrotron Radiation*; Ebashi, S., Koch, M., Rubenstein, E., Eds.; Elsevier: Amsterdam, 1991.
(10) Kjaer, K. *Physica B* **1994**, *198*, 100.
(11) Als-Nielsen, J.; Jaquemain, D.; Kjaer, K.; Lahav, M.; Leveiller, F.; Leiserowitz, L. *Phys. Rep.* **1994**, *246*, 251.
(12) Brezesinski, G.; Dietrich, A.; Struth, B.; Böhm, C.; Bouwman, W. G.; Kjaer, K.; Möhwald, H. *Chem. Phys. Lipids* **1995**, *76*, 145.
(13) Tippmann-Krayer, P.; Möhwald, H. *Langmuir* **1991**, *7*, 2298.
(14) Kenn, R. M.; Böhm, C.; Bibo, A. M.; Peterson, I. R.; Möhwald, H.; Als-Nielsen, J.; Kjaer, K. *J. Phys. Chem.* **1991**, *95*, 292.
(15) Böhm, C.; Möhwald, H.; Leiserowitz, L.; Kjaer, K.; Als-Nielsen, J. *Biophys. J.* **1993**, *64*, 553.
(16) Möhwald, H. *Rep. Prog. Phys.* **1993**, *56*, 653.
(17) Kaganer, V. M.; Loginov, E. B. *Phys. Rev. E* **1995**, *51*, 2237.
(18) Albrecht, O.; Gruler, H.; Sackmann, E. *J. Phys.* **1978**, *39*, 756.
(19) Lowack, K.; Helm, C. A. *Adv. Mater.* **1995**, *7*, 155.
(20) Chi, L. F.; Anders, M.; Fuchs, H.; Johnston, R. R.; Ringsdorf, H. *Science* **1993**, *259*, 213.
(21) Dautzenberg, H.; Hartmann, J.; Grunewald, S.; Brand, F. *Ber. Bunsenges. Phys. Chem.* **1996**, *100*, 1024.

MA961490B